

# Ray Tracing Modified 3D Image Method Simulation of Picocellular Propagation Channel Environment

F. Alwafie

**Abstract**—In this paper, we present the simulation of the propagation characteristics of the picocellular propagation channel environment. The first aim has been to find a correct description of the environment for received wave.

The result of the first investigations is that the environment of the indoor wave significantly changes as we change the electric parameters of material constructions. A modified 3D ray tracing image method tool has been utilized for the coverage prediction. A detailed analysis of the dependence of the indoor wave on the wideband characteristics of the channel: root mean square (RMS) delay spread characteristics and Mean excess delay, is also investigated.

**Keywords**—Propagation, Ray Tracing.

## I. INTRODUCTION

WAVE propagation in indoor environments in the UHF wave range are growing their importance day after day, becoming fundamental for the characterization of indoor propagation and it is well understood and can be modeled with ray tracing algorithms [1], [2]. The accurate design of a channel model still remains problematic, since the study of influence of some variable parameters are worth to avoid many problems for designing the microcellular wireless local area networks (WLANs). Therefore it is necessary to perform a deep optimization on the algorithm and simplifying assumptions on the propagation models are often unavoidable to increase performances. For our purposes, the classical ray tracing image method [15] was modified and the visible window image model (VWIM) of ray tracing was performed to analysis and simulated the propagation characteristics of the picocellular propagation channel environment [17]. The main point of the model was originally conceptualized from [4], to extend the 2D of the classical image method algorithm to the 2.5D in order to give more precision, and to reduce the computation time execution than 3D ray path. The advantage of that to make algorithm as 3D in accuracy and faster as 2D, and by this condition the optimization is realized, so that the channel profiles obtained by our method (VWIM) match sufficiently closely the measured data. Exhaustive simulations were then performed with (VWIM) ray tracing and the output data were analyzed.

The main elements in the scenarios that are partitions walls, ceilings, and floors are normally a combination of several

materials, forming different structures. The propagation of waves through such structures is a complex process that cannot be rigorously analyzed within a general-purpose program. Therefore, simple models of these structures are necessary to calculate transmitted, reflected, and diffracted fields by means of closed form expressions. The ray interactions with propagation environment are tracked for horizontal polarization and vertical polarization by taking into account the electromagnetic properties of construction materials [3].

## II. RELATED WORK

The classical image method [7], [16] were the algorithm starts by constructing an image or a projection of the transmitter in all the building surfaces visible to the transmitter. Then the secondary images of the different primary images are constructed on all the surfaces visible to the primary images. It is increasing the time computation, and this is clearly appeared at the model, were presented in [10], which using the 3D algorithm, were includes all possible specular reflections from the wall and ground reflections only and corner diffractions in the streets. This model used,  $\epsilon_r=15$  and  $\sigma=7$ , and up to 26 wall reflection points and 1 ground reflection are assumed for 3D model. In the model, as in [12], were 3D image method is proposed, and used “approximated illumination area algorithm”, with considered 2 reflections and one diffraction edge. There is evaluation area with a reflection objects are considered, and the evaluation area is filled with evaluation points which are equally spaced each other and they have same height. A ray reflected by the object may launch at a point in one of the evaluation points, also rays are launched at evaluation points within an “illuminated area” on the evaluation plane.

The illuminated area can be derived from the coordinates of the reflection object and the transmitter location and it is enough to trace the rays reflected by the object at evaluation points within the illuminated area [12]. In order to avoid such cumbersome coordinate calculations and to be able to treat illumination area regardless of the reflection order, only last imaging point is used to solve the “approximated illumination area” on the evaluation plane. Not all evaluation points within the approximated illumination area have the actual ray path due to this modification. Therefore, determination whether each points in the area has actual path or not is needed. The coordinates of the last imaging point and the vertices of the last reflected object can solve the approximated illumination area. The model algorithm [12] is developed by [13], where also 3D ray tracing model is proposed (image method) but

F. Alwafie is with the Faculty of Science Engineering & Technology, Sebha University (e-mail: fathi\_alwafi@yahoo.com).

here the diffracted from edges are included, the model divides illumination area into sectors, where constructing ray paths and checking their validity, the process can be decomposed into a horizontal and vertical sweep. The horizontal sweep checking the validity of an observation point, will involve tracing from that observation point back to the transmitter to ensure that the wall reflections are valid. If any point on the sector is horizontally invalid, then all points in the sector will be invalid, so that only point needs to be checked. In the case of the vertical sweep, the ray path is unfolded to show the route that the path takes in the plane. In the case of an image sector, the algorithm [13] define these angles by considering the first grid point in the sector, ray tracing back to the transmitter, recording the wall top and bottom edge elevation angles with respect to the image. For calculation the field strengths, it begin at the transmitter, so the computing the field at all observation points in the coverage area. Since the coverage area is defined to be a rectangular grid, it follows that the perimeter is automatically discretized according to the grid step size of this grid. In the model [13], has been accomplished by taking advantage of the fact that the ray tracing process can be decomposed into a horizontal 2D component and vertical 2D component. The algorithm, presented in [13] shows the accuracy and save more computation time, but the total computation time is proportional to the total number of grid points, and this can be expensive for a dense grid over a large area, and this indicted were the computation time for calculation was approximately 32 min. The SBR/Image method [9], [10] is the algorithm, which finds equivalent sources (images) for each lunched triangular ray tube. Where the triangular ray tubes are shot from Tx in the way to the Rx, and trace each ray tube, which bounces in the plan, and this method, used the theory of geodesic domes [7]. The SBR/Image model seems to be less rigorous than models based on classical image model, and accuracy depends on the radius of the reception sphere. In the beam tracing algorithm [8], [11], replaces the ray with beams that are represented as cones with polygonal cross sections. The beam consists of a collection of rays originating from a transmitter (or an image of the transmitter) and reflected or transmitted from a planar polygon.

The Beam tracing algorithm assumes that all the surfaces in the environment are represented as planar polygons. The beams are tested for intersection with the various surface elements in the environment. The polygons that represent the environment are first sorted according to the distance from the beam. The beam intersection tests are carried out with the nearest polygon first. An image of the transmitter is first computed by reflecting the transmitter through the plane of the polygon.

### III. SIMULATION METHODOLOGY

In the algorithm, the 2D of the classical image method algorithm was modified to the 2.5D in order to give more precision, and to reduce the computation time execution than 3D ray path algorithm [14]. The advantage of this idea to

make algorithm as 3D in accuracy and faster as 2D, and by this condition the optimization is realized. The main idea of algorithm was originally conceptualized from [4], were realized by ray launching method for outdoors environment, and scanning the ray path in the 2.5D, which means that when the ray path reflected from ceiling, and / or from ground can be uniquely represented by 3D coordinates: x, y, and z, and all reflections from the walls represented by 2D coordinates: x and y [14], [17]. Only one order ray reflection from the ceiling and one order ray reflection from ground are assumed, as shown in Fig. 1, which clearly show the 2.5D path emitted from Tx to the Rx and presented by black ray color.

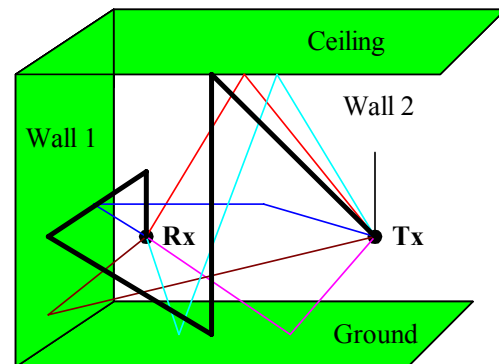


Fig 1 Rays in 2.5 dimensional space

### VI. SIMULATION SCENARIO

The algorithm is implemented by using C++ Builder language. The model was applied to the room laboratory, which has dimension (5.5m wide, 6m length, and 2.6m height), as indicated in Fig. 2. The location of transmitter (Tx) was stationary, and a total twelve receiver positions selected as Rx1, Rx2, up Rx12, and as shown in Fig. 2. The simulation were performed for frequency of 1.9GHz, the walls of room are made of concrete, which has dielectric constant ( $\epsilon = 7+j0.4$ ), and there are two doors, one made of wood, which has dielectric constant ( $\epsilon = 2.5+j0.03$ ), and second made of metallic, and has dielectric constant ( $\epsilon = 1+j0.0$ ). The partial of wall covered with glass windows, which has dielectric constant ( $\epsilon = 6+j0.05$ ).

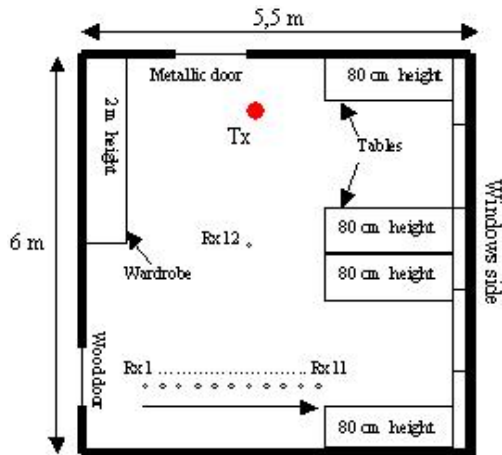


Fig. 2 Schematic of Lab room were the predicted results for 12 location of receiver

Fig. 3 shows the visible rays received by receiver (Rx1) inside room and Table I shows the visible window images, which detected by receiver location (Rx1) for different mode of VWIM algorithm, were 5 reflections are used, and clearly show us that the 2.5D mode produces a compromise between the 2D and 3D mode, and can reducing the algorithm process about 50% than 3D. Tables II and III show values for the mean excess delay ( $\tau$ ), and RMS delay spread ( $\sigma$ ) for each receiver locations for line of sight (LOS) and non line of sight (NLOS) situation respectively inside Lab room as mentioned in Fig. 2. The average RMS delay spread of LOS twelve receiver locations was 11.25ns for measured and 10.20ns for 2.5D simulation, and the average RMS delay spread for the same locations but for NLOS, was 14.42ns and 30.02ns for measured and simulated situation respectively, while for 2D is 10.63ns and 11.57ns for 3D case. The average RMS delay spread for the same receiver locations but for NLOS, was 10.65ns, 10.53ns, and 12.07ns for 2.5D, 2D, and 3D simulated situation respectively, and 9.24ns for measured result. Some predicted results are agree with measured results and some

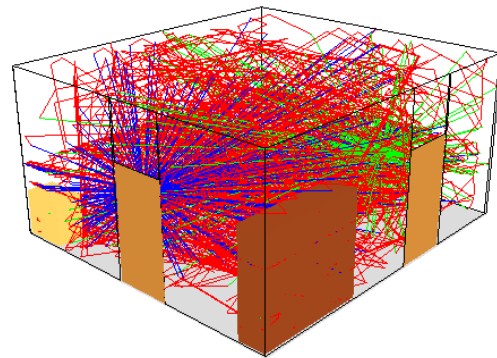


Fig. 3 Visible rays received by receiver inside room

TABLE I  
VISIBLE RAYS DETECTED AND REALIZED BY VWIM MODEL

| Mode | Number of Reflections | Visible Rays | Total Rays | Received Rays |
|------|-----------------------|--------------|------------|---------------|
| 3D   | 5                     | 8115785      | 1937       | 342           |
| 2.5D | 5                     | 4726848      | 741        | 146           |
| 2D   | 5                     | 5264155      | 445        | 83            |

TABLE II  
RMS DELAY SPREAD AND MEAN EXCESS DELAY FOR RECEIVER LOCATIONS INSIDE LAB ROOM FOR LOS CASE

| Location<br>LOS Inside LAB Room | Measured      |             | RayProp Simulation Optimization Mode |             |               |             |               |             |
|---------------------------------|---------------|-------------|--------------------------------------|-------------|---------------|-------------|---------------|-------------|
|                                 | $\sigma$ [ns] | $\tau$ [ns] | 2D                                   |             | 2.5D          |             | 3D            |             |
|                                 |               |             | $\sigma$ [ns]                        | $\tau$ [ns] | $\sigma$ [ns] | $\tau$ [ns] | $\sigma$ [ns] | $\tau$ [ns] |
| Rx1                             | 8.88          | 19.70       | 10.32                                | 19.92       | 10.20         | 21.27       | 11.35         | 22.93       |
| Rx2                             | 10.09         | 20.21       | 10.57                                | 19.97       | 10.32         | 21.49       | 11.43         | 22.91       |
| Rx3                             | 14.55         | 29.99       | 10.49                                | 19.43       | 10.52         | 21.52       | 11.67         | 23.34       |
| Rx4                             | 10.21         | 20.21       | 9.94                                 | 20.15       | 9.99          | 21.11       | 11.05         | 22.62       |
| Rx5                             | 8.96          | 22.29       | 9.76                                 | 19.47       | 9.31          | 20.27       | 10.60         | 21.80       |
| Rx6                             | 10.23         | 21.00       | 10.27                                | 19.68       | 9.64          | 20.37       | 11.05         | 22.03       |
| Rx7                             | 13.98         | 23.38       | 10.86                                | 18.29       | 10.41         | 20.15       | 11.80         | 21.91       |
| Rx8                             | 10.55         | 19.19       | 10.35                                | 19.84       | 10.35         | 20.10       | 11.91         | 22.07       |
| Rx9                             | 12.81         | 21.91       | 11.13                                | 18.58       | 10.35         | 20.23       | 11.96         | 22.19       |
| Rx10                            | 12.79         | 21.27       | 11.91                                | 20.67       | 10.25         | 20.85       | 11.45         | 22.59       |
| Rx11                            | 9.28          | 21.38       | 11.19                                | 20.80       | 9.63          | 20.83       | 10.92         | 22.39       |
| Rx12                            | 12.61         | 11.11       | 10.80                                | 12.30       | 11.51         | 15.26       | 13.62         | 18.37       |
| Average                         | 11.25         | 20.97       | 10.63                                | 19.09       | 10.20         | 20.29       | 11.57         | 22.10       |

TABLE III  
RMS DELAY SPREAD AND MEAN EXCESS DELAY FOR RECEIVER LOCATIONS INSIDE LAB ROOM FOR NLOS CASE

| Location<br>NLOS Inside LAB Room | Measured      |             | RayProp Simulation Optimization Mode |             |               |             |               |             |
|----------------------------------|---------------|-------------|--------------------------------------|-------------|---------------|-------------|---------------|-------------|
|                                  |               |             | 2D                                   |             | 2.5D          |             | 3D            |             |
|                                  | $\sigma$ [ns] | $\tau$ [ns] | $\sigma$ [ns]                        | $\tau$ [ns] | $\sigma$ [ns] | $\tau$ [ns] | $\sigma$ [ns] | $\tau$ [ns] |
| Rx1                              | 11.13         | 19.64       | 10.60                                | 20.30       | 10.43         | 21.55       | 12.77         | 23.72       |
| Rx2                              | 10.95         | 19.09       | 11.25                                | 21.21       | 12.08         | 22.71       | 13.00         | 24.54       |
| Rx3                              | 9.29          | 18.13       | 11.31                                | 20.38       | 11.62         | 22.63       | 12.56         | 24.29       |
| Rx4                              | 11.79         | 20.05       | 10.16                                | 21.22       | 11.31         | 22.32       | 12.30         | 24.01       |
| Rx5                              | 9.28          | 20.23       | 10.25                                | 20.44       | 10.50         | 21.52       | 11.63         | 23.19       |
| Rx6                              | 8.76          | 18.56       | 10.43                                | 19.95       | 10.31         | 21.34       | 11.49         | 22.96       |
| Rx7                              | 11.03         | 18.98       | 10.96                                | 18.57       | 10.89         | 20.99       | 12.04         | 22.81       |
| Rx8                              | 8.82          | 17.68       | 10.70                                | 18.41       | 10.59         | 20.69       | 12.08         | 22.66       |
| Rx9                              | 10.27         | 23.00       | 9.22                                 | 20.05       | 9.49          | 20.67       | 11.12         | 22.36       |
| Rx10                             | 4.92          | 20.42       | 10.39                                | 19.56       | 9.59          | 20.77       | 10.96         | 22.30       |
| Rx11                             | 3.84          | 20.42       | 10.28                                | 19.33       | 9.35          | 20.51       | 10.89         | 22.13       |
| Rx12                             | 10.76         | 9.28        | 10.85                                | 11.15       | 11.61         | 13.93       | 14.02         | 17.13       |
| Average                          | 9.24          | 18.79       | 10.53                                | 19.21       | 10.65         | 20.80       | 12.07         | 22.68       |

## V. CONCLUSION

In this paper, the efficient (VWIM) algorithm, were implemented by RayProp software package simulator, and released in the Lab room environment. The proposed model avoids the use of the usual time-consuming algorithms to determine the appropriate propagation paths. It therefore provides significant advantage in computational efficiency. A correlation study was performed for mean excess delay with respect to the receiver displacement. Excellent agreements were observed with compared with real measurement results with our model for the same test site. The study shows to use 2.5D mode properly useful for both LOS and NLOS than using 2D and 3D mode.

## REFERENCES

- [1] M. Lecours, D. Grenier, M. Baqarhi, and S. Cherkaoui, "Measurements and simulation of received signals in rooms and corridors at 900 MHz and in the 20–60 GHz band," in *Proc. VTC 1993*, 1993, pp. 871–874.
- [2] M. H. A. Ali, and K. Pahlavan, "Site-specific wideband indoor channel modelling using ray tracing software", *Electronic Lett.*, Vol.23, No.33, pp.1983–84, Nov 1997
- [3] Z. Chen, H. L. Bertoni, and A. Delis, "Progressive and approximate techniques in ray tracing based radio wave propagation prediction models", *IEEE Trans. Antennas and Propagation*, Vol. 52, No. 1, pp. 240–251, 2004.
- [4] F. A. Agelet, F. P. Fontán, and A. Formella, "Fast ray tracing for microcellular and indoor environments," *IEEE Transactions on Magnetics*, 33(2), March 1997, pp. 1484–1487.
- [5] S. Lored, L. Valle, and R. P. Torres, "Accuracy analysis of GO/UTD radio channel modeling in indoor scenarios at 1.8 and 2.5 GHz," *IEEE Antennas and Propagation Magazine*, vol. 43, no. 5, pp. 37–51, Oct 2001.
- [6] A. G. Smithson, "Wide area radio channel modeling across the indoor / outdoor interface," Ph.D. Dissertation, The University of Bath, Department of Electronic and Electrical Engineering, October 2005.
- [7] M. J. Wenninger, Spherical models, *Cambridge University Press*, New York, 1979.
- [8] Paul. S. Heckbert, and Pat. Hanrahan, Beam Tracing Polygonal Objects, In *SIGGRAPH '84*, page. 119–127, 1984.
- [9] S-H. Chen, and S-K. Jeng, "An SBR/image approach for radio wave propagation in indoor environments with metallic furniture," *IEEE Transactions Antennas and Propagation*, vol. 45, no. 1, pp. 98–106, Jan 1997.
- [10] S-H. Chen, and S-K. Jeng, "An SBR/image approach to indoor radio propagation modelling," in *IEE Antennas and Propagation Society International Symposium*, 1995 Digest, June 1995, vol. 4, pp. 1952–1955.
- [11] S. Fortune, "Efficient algorithms for prediction of indoor radio propagation," *IEEE Vehicular Technology Conference*, vol. 1, pp. 572–576, 1998.
- [12] T. S. Rappaport, B. D. Woerner, and J. H. Reed, *Wireless Personal Communications: the evolution of personal communication systems*, Kluwer Academic Publishers, pp. 111–121, 1996.
- [13] W. M. O'Brien, E. M. Kenny, and P. J. Cullen, "An efficient implementation of a three dimensional microcell propagation tool for indoor and outdoor urban environments," *IEEE Transactions on Vehicular Technology*, vol. 49, no. 2, pp. 622–630, Marc 2000.
- [14] F. Alwafie, "2.5D model propagation paths inside building using ray tracing," ICECE, Dubai, pp. 27 – 30, Jan, 2011
- [15] T. Whitted, "An improved illumination model for shaded display," *ACM*, vol. 23, no. 6, pp. 343–349, 1980.
- [16] H. Sang Kim, "Measurement and model based characterization of indoor wireless channels," Ph.D. Dissertation, University of Massachusetts Lowell, 2003.
- [17] F. Alwafie, "Radaio wave propagation in picocellular environment using 2.5D ray tracing technique," <http://www.waset.org/journals/waset/v70/v70-18.pdf>.